Downregulation of IRS-1 Expression Causes Inhibition of Corneal Angiogenesis

Marianne Berdugo,[1,2] *Charlotte Andrieu-Soler,*[1,2,3] *Marc Doat,*[1] *Yves Courtois,*[1] *David BenEzra,*[4] *and Francine Behar-Cohen*[1,5]

Purpose. The antiangiogenic effect of an antisense oligodeoxynucleotide (ODN) targeting insulin receptor substrate (IRS)-1 was evaluated on rat corneal neovascularization.

Methods. Eyes with neovessels were treated with subconjunctival injections of IRS-1 antisense oligonucleotide (ASODN), IRS-1 sense ODN (SODN), or PBS. At 8 and 24 hours after the first subconjunctival injection, the expression of IRS-1, VEGF, and IL-1β mRNA was evaluated. IRS-1 protein levels were also measured at 8 hours by Western blot analysis ($n = 4$/group). On day 10, corneal neovascularization was quantified in flat-mount corneas of rats treated daily from days 4 to 9.

Results. On day 10, new vessels covered 95.5% $\pm$ 4% of the corneal area in PBS-treated eyes, 92% $\pm$ 7% in SODN-treated eyes and 59% $\pm$ 20% in ASODN-treated eyes ($P < 0.001$). In the ASODN-treated group, the expression and synthesis of IRS-1 were significantly downregulated when compared with the control groups. ASODN did not significantly affect the expression of VEGF but significantly decreased the expression of IL-1β at 24 hours ($P = 0.04$).

Conclusions. Subconjunctival injections of IRS-1 antisense ODN significantly inhibit rat corneal neovascularization. This effect may be mediated by a downregulation of IL-1β. IRS-1 proteins may be interesting targets for the regulation of angiogenesis mediated by insulin, hypoxia, or inflammation. (*Invest Ophthalmol Vis Sci.* 2005;46:4072–4078) DOI:10.1167/iovs.05-0105

Antisense oligonucleotides (ODNs) displaying base sequences complementary to a specific mRNA are able to modulate the expression of specific genes.[1] This approach was investigated for the treatment of viral infections and cancer.[2–5] The antisense strategy is particularly attractive for the treatment of ocular disease. The eye is a small and closed organ in which an applied drug remains locally available with limited systemic diffusion. The first FDA-approved antisense ODN was for the treatment of cytomegalovirus (CMV) retinitis. Pathologic neovascularization of ocular tissues is one of the major causes of vision impairment and blindness worldwide. Therefore, antiangiogenic strategies are being extensively explored in various experimental designs. Phosphorothioate antisense ODNs directed at bFGF have been shown to inhibit corneal neovascularization in the rat.[6]

Insulin receptor substrates (IRSs) are cytosolic adapter proteins that do not contain intrinsic kinase activity but recruit proteins to surface receptors and induce organization of signaling complexes. IRS-1 was originally isolated as an insulin receptor substrate. However, it has since been shown to play a wider role, functioning as a proximal substrate in growth hormones and cytokine receptor signaling.[7–9] The vascular insulin-like growth factor system has been implicated in several vascular diseases, including angiogenesis.[10] Its role in angiogenesis may be mediated by regulation of vascular endothelial growth factor (VEGF)[11,12] and/or by other proangiogenic cytokines,[8] as well as by interactions with integrins. Insulin increases the expression of VEGF in retinal pigment epithelial cells,[13] transformed cells,[14] and vascular endothelial cells.[12] In the neonatal mouse model of hypoxia-induced retinal neovascularization, the growth of pathologic vessels was reduced in IRS-$1^{-/-}$ mice, suggesting that IRS-1 may play an important role in the development of retinal neovessels.[12] In tubular kidney epithelial cells, binding of VEGF to its type 2 receptor promotes the association of IRS-1 with the VEGF-receptor complex.[15] Another property of IRS proteins is their ability to associate with integrins, which may intervene in the regulation of cell growth and/or transformation.[16] Taken together, these observations indicate that IRS-1 may be an interesting regulatory molecule during the development of ocular neovessels.

The avascular clear cornea allows for easy observation and monitoring of induced angiogenesis and direct access to treatment of the emerging new vessels. In corneal models of neovascularization, VEGF, cytokines, and interleukins are known to play central roles.[17–19] IL-1β has been shown to be one of the most potent angiogenic cytokines, inducing corneal neovascularization accompanied by infiltration of inflammatory cells.[17] It has also been demonstrated that IL-1β has particularly potent proangiogenic activity, and its inhibition suppresses neovascularization in tumors[20] and in a corneal model.[19] More recently, it was suggested that IL-1β proangiogenic activity is mediated through angiopoetin-1 downregulation, both in endothelial cells and in pericytes.[21]

The purpose of the present study was to evaluate the potential antiangiogenic effect of an antisense ODN directed at IRS-1 on corneal neovascularization in the rat. The effect of IRS-1 downregulation on VEGF and IL-1β expression was also investigated.

Materials and Methods

Animals

All experiments in this study were conducted in accordance with the ARVO Statement for the Use of Animals in Ophthalmic and Vision Research and the institutional guidelines regarding animal experimentation.

Eighty-eight male Lewis rats, 5 weeks old, specific pathogen free, and weighing 185 $\pm$ 25 g were used (Charles River France, St-Aubin les

From the [1]Institut National de la Santé et de la Recherche Médicale (INSERM), U598, Paris, France; [3]Optis France, Paris, France; [4]Hadassah Hebrew University Hospital, Jerusalem, Israel; and the [5]Rothschild Foundation, Paris, France.

[2]Contributed equally to the work and therefore should be considered equivalent authors.

Supported in part by Gene Signal, Evry, France.

Submitted for publication January 27, 2005; revised April 29, and June 7, 2005; accepted August 29, 2005.

Disclosure: **M. Berdugo**, None; **C. Andrieu-Soler**, Optis France (E); **M. Doat**, None; **Y. Courtois**, None; **D. BenEzra**, None; **F. Behar-Cohen**, None

The publication costs of this article were defrayed in part by page charge payment. This article must therefore be marked "*advertisement*" in accordance with 18 U.S.C. §1734 solely to indicate this fact.

Corresponding author: Francine Behar-Cohen, INSERM U598, Institut Biomédical des Cordeliers, 15 rue de l'Ecole de Médecine, 75006 Paris, France; behar@idf.inserm.fr.

Elbeufs, France). Before experimentation, animals were anesthetized by intramuscular injection of ketamine chlorohydrate 125 mg/kg (UVA, Ivry sur Seine, France) and chlorpromazine 5 mg/kg (Specia Rhône Poulenc, Paris, France). At the end of the experiments, rats were killed with an overdose of pentobarbital sodium (Ceva Santé Animale, Libourne, France).

Oligonucleotides

Phosphorothioate antisense and sense ODNs were designed and synthesized (Eurogentec, Herstal, Belgique) to include the translation start site of IRS-1. The sequences were 5′-TATCCGGAGGGCCTGCCATGCT-GCT-3′ for the antisense and 5′-AGCAGCATGGCAGCCCTCCGGATA-3′ for the sense ODN.[22] ODNs were diluted in 1× PBS (pH 7.2; 60 μM) for subconjunctival injections.

Corneal Neovascularization

Only the right eye of each rat was used. Neovascularization was induced by mechanical resection of the corneal epithelium and limbal debridement, as previously described by Amano et al.[18] Briefly, the corneal epithelium was mechanically removed with a surgical microsponge imbibed with 70% alcohol. In addition, a 1.5-mm wide strip of conjunctiva was excised around the limbus with microscissors. At the end of surgery, a suture tarsorrhaphy (5-0 silk) maintained the eyelids closed until day 4.

Quantification of Neovascularization

On days 4 (initiation of subconjunctival treatment), 7, and 10, the evolution of new corneal vessels was examined clinically with a biomicroscope (BQ900; Haag Streit, Wedel, Germany). For quantification of corneal neovessels on day 4 (4 rats) or 10 (18 rats), the animals were killed and perfused with fluorescein-dextran 2×10^6. The eyes were then enucleated and fixed in 4% paraformaldehyde for 3 hours and rinsed in 1× PBS. The corneas including 1 mm of sclera were dissected, flatmounted in a solution of PBS-glycerol (1:1), examined under a fluorescence microscope (Leica, Wetzlar, Germany), and photographed. The corneal areas of neovascularization were quantified with NIH Image software (ver.1.62; available by ftp at zippy.nimh.nih.gov/ or at http://rsb.info.nih.gov/nih-image; developed by Wayne Rasband, National Institutes of Health, Bethesda, MD). For each whole cornea, the mean of three measurements was recorded. The area of neovascularization was expressed as a percentage of total corneal area. The corneal neovessels from control and treated rats were also examined by inverted confocal fluorescence microscope (LSM 510; Carl Zeiss Meditec, Oberkochen, Germany) and a 488-nm argon laser.

Experimental Design

Four rats without neovessels were killed 1 hour after subconjunctival injection of a labeled ODN, to evaluate its distribution in the anterior segment of the eye.

To assess the optimal antisense oligonucleotide (ASODN) concentration to be used for the study, 18 rats ($n = 6$/concentration) with corneal neovascularization received, from days 4 to 9, daily subconjunctival injections of 0.6, 6, or 60 μM in 50 μL of PBS. To avoid the potential secondary toxic effect of phosphorothioate, ODN concentrations higher than 60 μM were not evaluated. Areas of neovascularization were quantified on flatmount corneas on day 10, as previously described. The group treated with 60 μM concentration showed the highest inhibitory effect. This concentration was therefore used for all additional experiments, as described in the following sections.

Growth of neovessels was induced in 66 rats as described, 8 of which were killed before any treatment was applied, for quantification of neovascularization and evaluation of inflammatory cell infiltration on day 4 (on opening of the tarsorrhaphy). The other 54 rats were divided into three treatment groups ($n = 18$/group) receiving subconjunctival injections of PBS (50 μL), sense ODN (SODN) in PBS (50 μL, 60 μM), or ASODN in PBS (50 μL, 60 μM). Injections were performed with a 30-gauge needle, in the inferotemporal subconjunctival space in rats under topical anesthesia (bupivacaine drops; Novesine, Chibret, France).

In each group, the 18 rats were divided as follows: six rats received one subconjunctival injection daily from days 4 to 9 and were assayed for quantification of neovascularization on day 10. Eight rats were used for reverse transcription–polymerase chain reaction (RT-PCR) analysis at 8 and 24 hours after the first injection ($n = 4$/time point). Four rats were used for Western blot analysis at 8 hours after the first injection.

Four additional ASODN-treated rats were used for the evaluation of cells ($ED1^+$) infiltrating the neovascularized corneas before and after treatment. Two rats were killed and their corneas tested on day 4 (before initiation of the subconjunctival injections of ASODN) and two rats were killed and their corneas tested on day 10 (24 hours after the last treatment).

Distribution of Oligonucleotide after Subconjunctival Injection

To evaluate the distribution of ODN, we injected four rats (without corneal neovascularization) in the subconjunctival space with 50 μL of either PBS ($n = 2$) or fluorescent (FITC) ASODN (60 μM; $n = 2$). Rats were killed at 1 hour after the injection, and the eyes were embedded in optimal cutting temperature (OCT) compound (Tissue-Tek; Sakura, Zoeterwoude, The Netherlands), snap frozen, and cryosectioned (7-μm thick). After washings (three times, 5 minutes each), nuclei were stained with 1:1000 diamino-2-phenylindol (DAPI) for 2 minutes, rinsed (three times, 5 minutes each) in PBS and mounted in glycerol/PBS (50/50) for direct fluorescence microscopy. Slides were examined with a fluorescence microscope (Leica) coupled to a digital camera (SPOT; Optilas, Evry, France).

Expression of IRS-1, VEGF, and IL-1β in Rat Corneas

At 8 and 24 hours after the first subconjunctival injection, expressions of IRS-1, VEGF, and IL-1β mRNA were evaluated by semiquantitative RT-PCR.

Total RNA was prepared from freshly dissected corneas (RNeasy Minikit; Qiagen, Les Ulis, France). Each RNA sample was obtained from a single cornea. First-strand cDNA was generated by reverse transcription of 100 ng total RNA with oligo dT (Invitrogen, Cergy Pontoise, France) with MMLV-reverse transcriptase, according to the instructions of the supplier (Invitrogen). This process yielded 20 μL cDNA, of which 1 μL was used for each semiquantitative PCR analysis. The cDNAs were amplified in a 50-μL reaction volume containing 20 mM Tris-HCl (pH 8.4), 50 mM potassium chloride, 1.5 mM magnesium chloride, 0.2 mM of each of the dNTPs, 0.5 μM of each appropriate primers (IRS-1 forward 5′-AAGTG-GCGGCACAAGTCGAG-3′, reverse 5′-CGGGTGTAGAGAGCCACCAG-3′; VEGF forward 5′-CCTGGTGGACATCTTCCAGGAGTACC-3′, reverse 5′-GAAGCTCATCTCTCCTATGTGCTGGC-3′, IL-1β forward v5′-TGTTTGG-GATCCACACTCTC-3′, reverse 5′-TTCCCATTAGACAGCTGCAC-3′; and glyceraldehyde-3-phosphate dehydrogenase (GAPDH) forward 5′-ACCA-CAGTCCATGCCATCAC-3′, reverse 5′-TCCACCACCCTGTTGCTGTA-3′) and 1.25 U *Taq* polymerase (Invitrogen). PCR in its exponential phase consisted of 1 cycle denaturation for 30 seconds at 95°C followed by 35 cycles (IRS-1 and IL-1β), 28 cycles (VEGF), or 25 cycles (GAPDH) of (denaturation for 30 seconds at 95°C; annealing for 30 seconds at 55°C [VEGF and IL-1β] or 60°C [IRS-1 and GAPDH]; and DNA extension for 1 minute at 72°C) and a final DNA extension at 72°C for 7 minutes. Each PCR reaction was performed in triplicate. Experiments were reproduced three times. IRS-1, VEGF, IL-1β, and GAPDH PCR products were separated on 1.5% agarose gels, with ethidium bromide used for visualization, and yielded the expected amplicon sizes of 112, 496, 195, and 451 bp, respectively. Band intensities were quantified with NIH Image software (ver. 1.57). Expression levels of the GAPDH gene were used for standardization. Results are expressed as the ratio of specific gene/GAPDH expression.

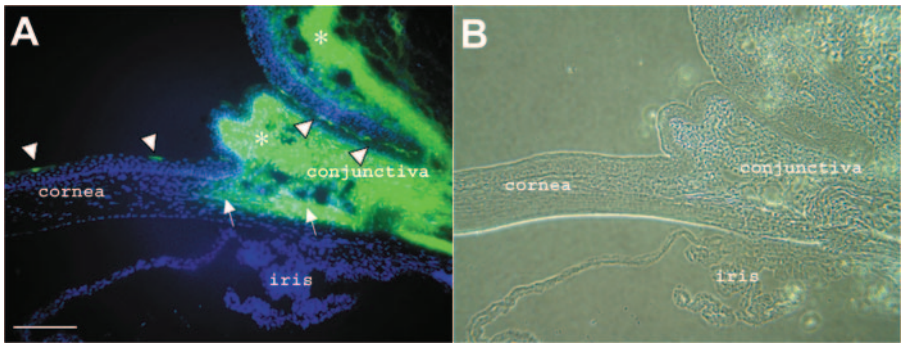

FIGURE 1. Distribution of fluorescent oligonucleotide 1 hour after subconjunctival injection. (**A**) Section of the eye anterior segment. Fluorescent ODN is observed in cells of the corneal and conjunctival epithelium (*arrowheads*), in the corneal stroma at the periphery near the limbus (*arrow*). (**B**) Same section in phase-contrast microscopy (same magnification). Scale bar, 500 μm.

Western Blot Analysis of IRS-1 in the Corneas

Production of IRS-1 protein was evaluated by Western blot at 8 hours after the first treatment. Two corneas from the same treatment group were pooled. Freshly dissected corneas were dissolved in ice-cold lysis buffer (10 mM Tris HCl [pH 7.5], 150 mM NaCl, 1 mM EDTA, 1 mM EGTA, 0.5% NP-40, and 1% Triton) with a protease inhibitor complex (Roche Diagnostics, Meylan, France). Protein concentrations were determined with the protein assay reagent (Bio-Rad, Marnes la Coquette, France), according to the Bradford method. Equal amounts of the solubilized proteins (20 μg) were mixed with 3× Laemmli buffer, heated for 5 minutes at 95°C, separated on 10% SDS-PAGE under reducing conditions, and transferred onto polyvinylidene (PVDF) membranes (Immobilon; Millipore, Saint-Quentin en Yvelines, France). The membranes were blocked with 5% dry milk in TBS for 1 hour at 37°C, incubated with 1:100 primary polyclonal rabbit antibody against IRS-1 (Upstate Cell Signaling, Wolverton Millsouth, UK) in TBS-0.1% Tween 20 containing 1% dry milk for 1 hour at room temperature. After being washed five times for 5 minutes each in TBS-0.1% Tween 20 containing 1% dry milk, the membranes were incubated with a specific secondary antibody horseradish peroxidase-conjugated immunoglobulin G (GE Healthcare, Orsay, France) in TBS-0.1% Tween 20 containing 1% dry milk for 1 hour at room temperature. After the membranes were washed, they were analyzed by the enhanced chemiluminescence system according to the manufacturer's protocol (GE Healthcare). β-Actin was then detected by using a 1:150 goat polyclonal anti-β-actin (Tebu-bio; Le Perray en Yvelines, France) as the primary antibody with the aforementioned methods. All experiments were reproduced three times. Band intensities were quantified with NIH Image (ver. 1.57). Levels of β-actin production were used for standardization. Results were expressed as the ratio of IRS-1/β-actin production.

ED1 Immunohistochemistry

Eyes were enucleated and fixed in 4% paraformaldehyde for 1 hour, embedded in OCT compound (Tissue-Tek; Sakura) and cryosectioned (7 μm thick). Sections were rinsed with PBS and incubated in 1% Triton X-100 (Sigma-Aldrich) PBS for 30 minutes. After the sections were washed with PBS, nonspecific fixation sites were saturated with 5% skimmed milk in PBS for 1 hour and then incubated at 4°C overnight with monoclonal mouse anti-rat ED1, to stain myeloid cells such as macrophages, according to the manufacturer's instructions (Serotec, Oxford, UK). Sections were then rinsed (three times, 5 minutes each) with PBS and incubated for 1 hour at room temperature with FITC anti-rabbit IgG (Molecular Probes, Inc., Eugene, OR) diluted (1:250) in PBS containing 1% BSA for 1 hour, then washed in PBS and mounted in PBS/glycerol (50:50).

Statistical Analysis

The area of neovascularization, measured on flatmounted cornea was expressed as a percentage of total corneal area. The mean ± SD of these ratios and normalized means of RT-PCR and Western blot analysis were compared between treatment groups by ANOVA, followed by a Bonferroni multiple-analysis posttest. $P < 0.05$ was considered as significant.

RESULTS

Distribution of Fluorescent Oligonucleotide 1 Hour after Subconjunctival Injection

After subconjunctival injection of the ODN preparation, intense fluorescence was observed in the conjunctival stroma, the limbus, and the corneal stroma periphery (Fig. 1). A few superficial epithelial cells of the cornea and of the conjunctiva also showed fluorescent labeling (arrowheads).

Effect of IRS-1 Antisense Oligonucleotide on Corneal Neovascularization

On opening of the tarsorrhaphy (day 4) and before any treatment was applied, a circular neovascularization of the corneas was clinically observed in all eyes. The new vessels progressed from the limbus 360° toward the center of the cornea. Quantification after dextran perfusion revealed that, at this stage, the extent of neovascularization was 43% ± 4% of the corneal area ($n = 4$). In the nontreated rats, on day 10, the extent of neovascularization was 95.5% ± 4% of the corneal area.

Neovascularization inhibition by the different concentrations of ASODN injections demonstrated a dose response. On day 10, injection of 0.6 μM had no significant inhibitory effect (percentage of neovascularized area 91.1% ± 2.6%, $P > 0.05$). Injection of 6 μM showed a low but significant reduction of the neovascularized area (83.9% ± 4.2%, $P < 0.01$), whereas in the group of rats treated with 60 μM the area of neovascularization was reduced to 59% ± 20% ($P < 0.01$).

On day 10, clinical examination of the corneas showed that in the ASODN-treated group, the area of neovascularization, the length and thickness of corneal vessels were reduced compared with the other two groups (Figs. 2A–C). Confocal microscopy of dextran-FITC–labeled flatmount corneas illustrates the reduced thickness of persisting neovessels in the ASODN-treated rats (Fig. 2F) compared with corneas from control groups (Figs. 2D, 2E). No toxic effect or local irritation due to the local administration of the ODNs was observed.

The percentage of corneal neovascularization, as measured on day 10 on flatmounted corneas, was 95.5% ± 4% and 92% ± 7% in the PB- and the SODN-treated groups, respectively. This result represents a 52% ± 0.4% and a 49% ± 0.9% increase in the neovascularization area compared with day 4 (Figs. 3A, 3B, 3D). In the group of rats treated with ASODN, the percentage of corneal neovascularization on day 10 was 59% ± 20%, an increased neovascularized area of only 16% ± 2% when compared to day 4 (Figs. 3C, 3D). When the ASODN-treated group was compared to either the SODN- or PBS-treated group, a

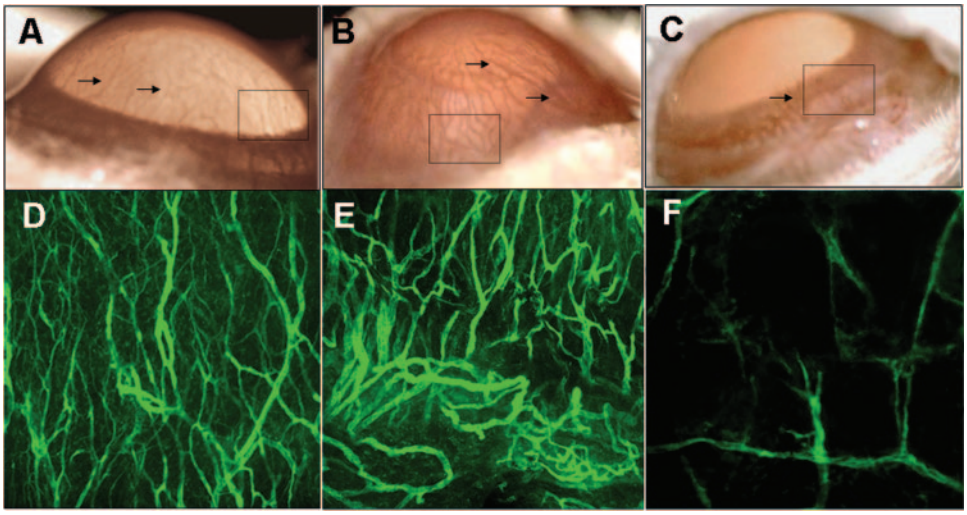

FIGURE 2. Effect of ASODN on corneal neovascularization at day 10. Slit lamp photographs of eyes from (**A**) PBS-, (**B**) SODN-, and (**C**) ASODN-treated rats. Fluorescent confocal images of flatmounted corneas from (**D**) PBS-, (**E**) SODN-, and (**F**) ASODN-treated rats injected with FITC-dextran. Magnification, ×50.

significant inhibition of neovascularization was observed ($P < 0.01$; Fig. 3D). No significant difference ($P > 0.05$) was observed in the percentage of corneal neovascularization between PBS- and SODN-treated rats (Fig. 3D).

Regulation of IRS-1, VEGF, and IL-1β mRNA Expression

RT-PCR analysis demonstrated that at 8 hours after ASODN injection, IRS-1 mRNA levels were reduced in the treated corneas by 60% when compared with the levels observed in corneas of rats treated with PBS ($P < 0.01$; Fig. 4). SODN had no effect on IRS-1 expression when compared with the PBS-treated group ($P > 0.05$; not shown). However, 24 hours after a single ASODN injection, RT-PCR did not show any sustained downregulation of IRS-1 mRNA production ($P > 0.05$; Figs. 5A, 5B), demonstrating that the ASODN downregulation was of short duration.

The expression of VEGF was not downregulated significantly in the group of rats treated with ASODN, when compared with either the SODN ($P > 0.05$)- or the PBS ($P > 0.05$)-treated groups at 8 hours or at 24 hours (Figs. 5A, 5C). However, at 24 hours, a significant downregulation of IL-1β was observed in ASODN-treated rats when compared with PBS ($P < 0.014$)- or SODN ($P < 0.001$; Figs. 5A, 5D)-treated rats. No significant difference in the level of IL-1β between PBS- and SODN-treated rats ($P > 0.05$) was observed.

Western Blot Analysis

Eight hours after the subconjunctival injection, the presence of IRS-1 protein was significantly reduced in the corneas of rats

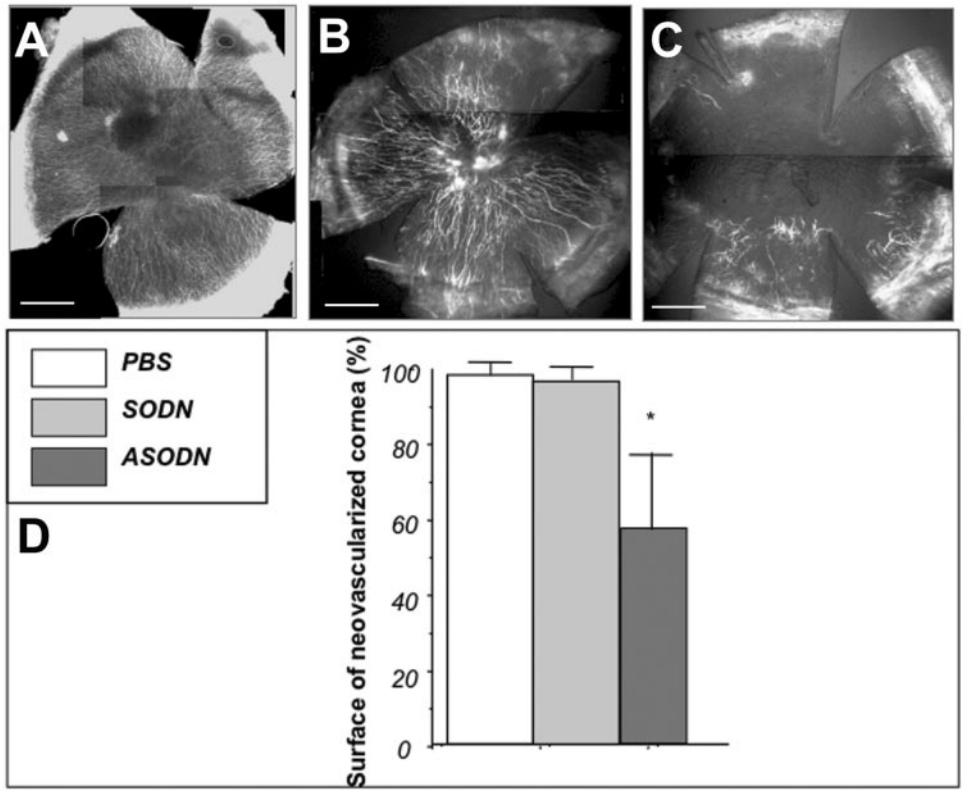

FIGURE 3. ASODN's effect on corneal neovascularization at day 10. Fluorescent photographs of whole flatmounted corneas from (**A**) PBS-, (**B**) SODN-, and (**C**) ASODN-treated rats injected with FITC-dextran. Scale bar, 1 mm. (**D**) Histogram representing mean percentages of cornea with neovascularization in the ASODN-treated and control groups. Results are expressed as the mean ± SD. The ASODN-treated group is significantly different from the SODN- and the PBS-treated groups (*$P < 0.01$).

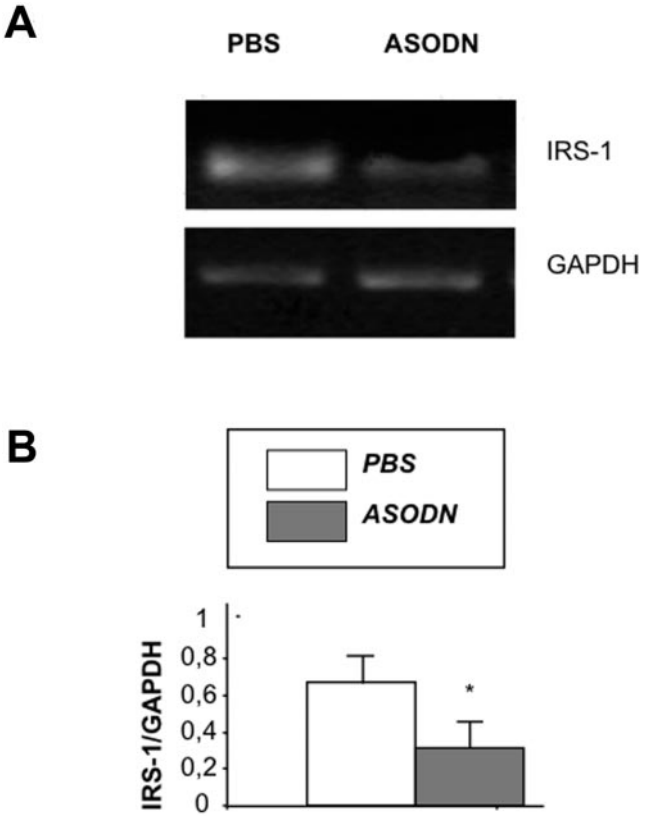

FIGURE 4. Effect of ASODN on IRS-1 expression 8 hours after treatment. (**A**) Ethidium-bromide–stained agarose gels representing RT-PCR products from PBS- and ASODN-treated corneas. (**B**) The ratio of semiquantitative RT-PCR of IRS-1/GAPDH in the PBS- and ASODN-treated groups. Results are expressed as the mean ± SD. The ASODN-treated group is significantly different from the PBS-treated group (*$P <$ 0.01).

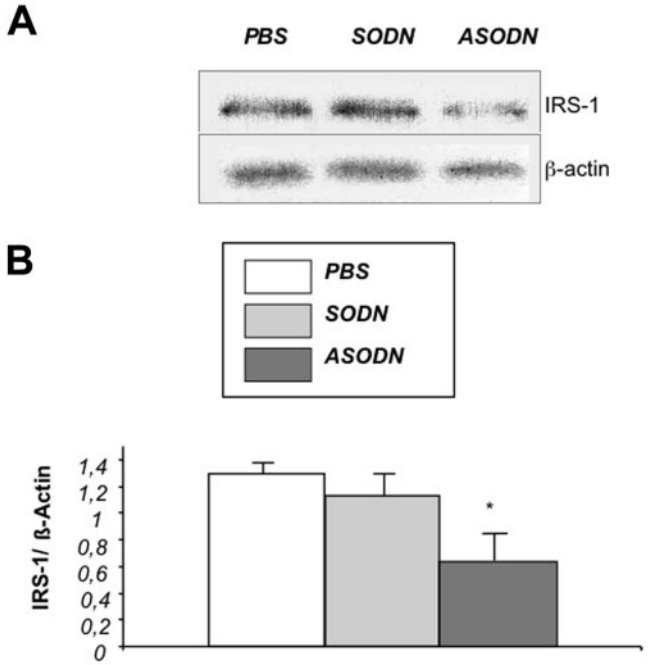

FIGURE 6. Effect of ASODN on IRS-1 protein production 8 hours after treatment. (**A**) Anti-IRS-1 and anti-β-actin Western blot gels from corneas of control, SODN- and ASODN-treated samples. (**B**) The ratio of IRS-1/β-actin proteins from control, SODN-, and ASODN-treated groups. Results are expressed as the mean ± SD. The IRS1 protein production in the ASODN-treated group is significantly different from that in either the SODN- or the PBS-treated groups (*$P <$ 0.01).

treated with ASODN when compared with the levels observed in corneas of rats treated with SODN or PBS (Fig. 6; $P < 0.01$ for both). The SODN had no effect on the production of IRS-1 when compared with the PBS-treated group ($P > 0.05$).

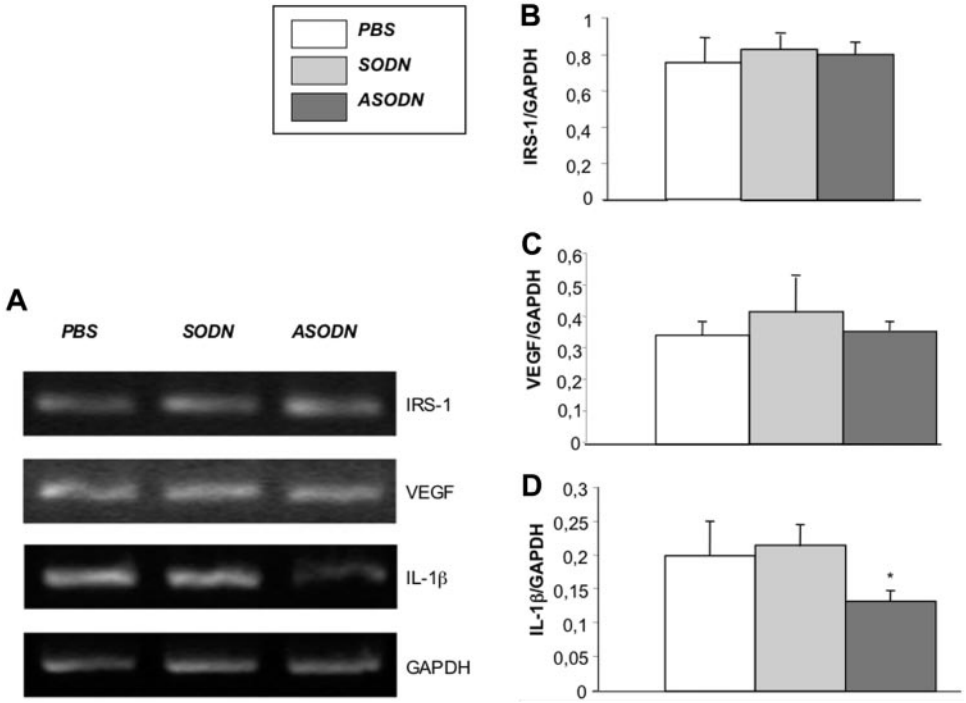

FIGURE 5. Effect of ASODN on IRS-1, VEGF, and IL-1β expression 24 hours after treatment. (**A**) Ethidium bromide–stained agarose gels representing RT-PCR products from PBS-, SODN-, and ASODN-treated eyes. Histograms show the ratios of semiquantitative RT-PCR of IRS-1/GAPDH (**B**), VEGF/GAPDH (**C**), and IL-1β/GAPDH (**D**). Results are expressed as the mean ± SD. The IL-1β expression in the ASODN-treated group is significantly different from that in either the SODN-treated group or the PBS-treated group (*$P <$ 0.01).

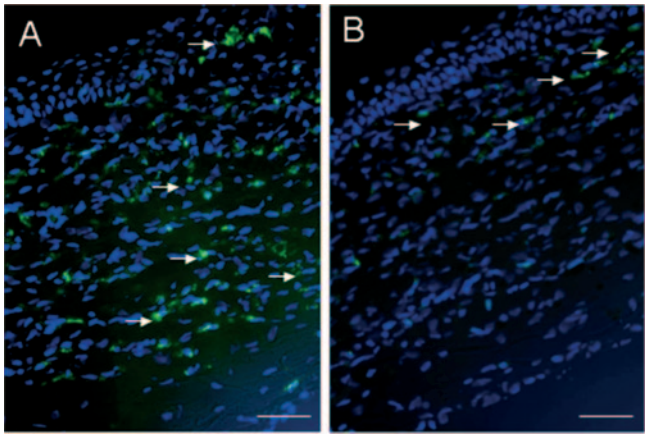

FIGURE 7. ED1 immunohistochemistry before and after ASODN treatment. (**A**) $ED1^+$ cells in cornea section costained with DAPI from an eye on day 4 (before treatment). (**B**) $ED1^+$ cells in cornea costained with DAPI from an eye on day 10 (24 hours after last ASODN treatment). *Arrows*: $ED1^+$ cells. Scale bar, 10 μm.

ED1 Immunohistochemistry

Figure 7 demonstrates that the corneas were massively infiltrated by macrophages on opening of the tarsorrhaphy and before initiation of treatment (Fig. 7A). In contrast, in the corneas of IRS-1 ASODN-treated rats, only occasional infiltrating cells were observed (Fig. 7B).

DISCUSSION

The inhibition of IRS-1 expression using a specific phosphorothioate antisense ODN efficiently reduced the growth of neovessels in the corneal model of neovascularization used in this study. A dose–response effect on the neovascularization was observed, with the highest effect (only 16% of additional neovessel growth) observed with the 60-μM concentration. No higher ODN dose was used, to avoid potential toxicity of phosphorothioate and related nonspecific effects.[23] The inhibition of neovascularization correlated well with the downregulation of both IRS-1 mRNA expression and protein levels in these corneas (and the number of infiltrating $ED\text{-}1^+$ cells). The specific antisense activity was also illustrated by the absence of effect of the SODN both on the growth of blood vessels observed clinically and on IRS-1 expression and production. From the distribution of ODNs after subconjunctival injection and their localization in the limbus and corneal stromal periphery, this route appears to be the most suitable for the targeting of vessel growth from the limbus toward the cornea center. Despite this potential advantage, the ODN subconjunctival injection, as performed in the present study, did not have a sustained downregulation effect.

The proangiogenic effect of IRS-1 has been demonstrated in a retinal model of neovascularization in the mouse.[12] The 40% reduction in retinal neovascularization observed in $IRS\text{-}1^{-/-}$ neonatal mice after hypoxia was interpreted to indicate that insulin may play a role on hypoxia-induced VEGF expression.[12] In corneal neovascularization models, angiogenesis is an integral part of the wound-healing response. VEGF has been recognized as one of the major proangiogenic cytokines in these processes. However, besides its ability to promote angiogenesis, VEGF has been identified as a principal permeability and proinflammatory mediator.[24,25] In our model, the specific inhibition of IRS-1 expression using a specific antisense ODN significantly reduced corneal angiogenesis without affecting VEGF expression. Similarly, in pancreatic cancer cells, Sp1-dependent VEGF transcription was not promoted by IRS-1, but it was promoted by IRS-2.[26]

In our model, IRS-1 downregulation significantly suppressed IL-1β expression in the treated corneas. IL-1β plays a major role in the promotion of inflammatory angiogenesis.[17,27–31] In tumors, IL-1β increased the production of proangiogenic factors, such as the macrophage inflammatory protein, CXCL2, the hepatocyte growth factor (HGF) and, to a lesser extent, the production of VEGF.[26] In contrast, the inhibition of IL-1β using a continuous delivery of IL-1β receptor antagonists was shown to reduce the development of tumors by decreasing the formation of blood vessels and the infiltration of inflammatory cells.[32] The reduction in the number of infiltrating macrophages may contribute, to the reduction in the production and release of NF-κB-dependent proangiogenic factors.[33] In our experiments, the inhibition of neovascularization in rats treated with IRS-1 ASODN was also associated with a decrease in the number of infiltrating macrophages. In corneal angiogenesis, IL-1β produced by infiltrating cells was shown to induce directly the growth of neovessels,[34] and the IL-1 receptor antagonist inhibited the growth of corneal neovessels.[19,28] Both in tumor and corneal angiogenesis, IL-1β inhibition is associated with antiangiogenic effects. Although the exact mechanism of its effect remains undetermined, there is ample evidence that IL-1β plays an important role in the promotion of angiogenesis. The specific and significant downregulation of IL-1β expression in the corneas of rats treated with IRS-1 ASODN, along with the absence of effect on VEGF expression suggests that, in this "inflammatory" model of corneal angiogenesis, several different processes may take place. The insulin-signaling pathway may act through NF-κB activation to regulate the expression of proangiogenic cytokines such as IL-1. This possibility has been demonstrated in keratinocytes.[35] Alternatively, other independent regulatory pathways may be responsible for VEGF expression.

More recently, IL-1β-induced angiogenesis was shown to be inhibited by COX2 inhibitors and not by VEGF inhibitors.[30] These findings and our own observations derived from the present study indicate that angiogenesis and antiangiogenic effects can take place without necessarily involving the VEGF production or inhibition.

Due to their possible implications in VEGF-mediated pathways and in permeability,[12,15,24,26] in cytokine-transduction pathways,[7,8,36–38] and in integrin interactions,[16,39,40] IRS proteins may be effective molecules for used in the modulation of angiogenesis triggered by hypoxia, insulin, or inflammation.

In the present study, IRS-1 reduced the extent of ongoing corneal neovascularization and thus opens new avenues for the potential treatment of ocular neovascular processes. Further studies are under way to elucidate the exact molecular mechanisms of IRS-1 proangiogenic effects in corneal angiogenesis.

References

1. Helene C, Toulme JJ. Specific regulation of gene expression by antisense, sense and antigene nucleic acids. *Biochim Biophys Acta*. 1990;1049:99–125.
2. Cohen JS. Antisense oligodeoxynucleotides as antiviral agents. *Antiviral Res*. 1991;16:121–133.
3. Crooke ST. Therapeutic applications of oligonucleotides. *Biotechnology*. 1992;10:882–886.
4. Milligan JF, Matteucci MD, Martin JC. Current concepts in antisense drug design. *J Med Chem*. 1993;36:1923–1937.
5. Orr RM. Technology evaluation: fomivirsen, Isis Pharmaceuticals Inc/CIBA Vision. *Curr Opin Mol Ther*. 2001;3:288–394.
6. Kitajima I, Unoki K, Maruyama I. Phosphorothioate oligodeoxynucleotides inhibit basic fibroblast growth factor-induced angiogenesis in vitro and in vivo. *Antisense Nucleic Acid Drug Dev*. 1999;9:233–239.

7. White MF. The insulin signalling system and the IRS proteins. *Diabetologia.* 1997;40(suppl 2):S2–S17.
8. White MF. The IRS-signaling system: a network of docking proteins that mediate insulin and cytokine action. *Recent Prog Horm Res*. 1998;53:119–138.
9. Shpakov AO, Pertseva MN. Structural and functional characterization of insulin receptor substrate proteins and the molecular mechanisms of their interaction with insulin superfamily tyrosine kinase receptors and effector proteins. *Membr Cell Biol*. 2000;13:455–484.
10. Delafontaine P, Song YH, Li Y. Expression, regulation, and function of IGF-1, IGF-1R, and IGF-1 binding proteins in blood vessels. *Arterioscler Thromb Vasc Biol*. 2004;24:435–444.
11. Miele C, Rochford JJ, Filippa N, Giorgetti-Peraldi S, Van Obberghen E. Insulin and insulin-like growth factor-I induce vascular endothelial growth factor mRNA expression via different signaling pathways. *J Biol Chem*. 2000;275:21695–21702.
12. Jiang ZY, He Z, King BL, et al. Characterization of multiple signaling pathways of insulin in the regulation of vascular endothelial growth factor expression in vascular cells and angiogenesis. *J Biol Chem*. 2003;278:31964–31971.
13. Slomiany MG, Rosenzweig SA. Autocrine effects of IGF-I-induced VEGF and IGFBP-3 secretion in retinal pigment epithelial cell line ARPE-19. *Am J Physiol*. 2004;287:C746–C753.
14. Bermont L, Lamielle F, Lorchel F, et al. Insulin up-regulates vascular endothelial growth factor and stabilizes its messengers in endometrial adenocarcinoma cells. *J Clin Endocrinol Metab*. 2001; 86:363–368.
15. Senthil D, Ghosh Choudhury G, Bhandari BK, Kasinath BS. The type 2 vascular endothelial growth factor receptor recruits insulin receptor substrate-1 in its signalling pathway. *Biochem J*. 2002; 368:49–56.
16. Vuori K, Ruoslahti E. Association of insulin receptor substrate-1 with integrins. *Science*. 1994;266:1576–1578.
17. BenEzra D, Hemo I, Maftzir G. In vivo angiogenic activity of interleukins. *Arch Ophthalmol*. 1990;108:573–576.
18. Amano S, Rohan R, Kuroki M, Tolentino M, Adamis AP. Requirement for vascular endothelial growth factor in wound- and inflammation-related corneal neovascularization. *Invest Ophthalmol Vis Sci*. 1998;39:18–22.
19. Yamada J, Dana MR, Sotozono C, Kinoshita S. Local suppression of IL-1 by receptor antagonist in the rat model of corneal alkali injury. *Exp Eye Res*. 2003;76:161–167.
20. Bar D, Apte RN, Voronov E, Dinarello CA, Cohen S. A continuous delivery system of IL-1 receptor antagonist reduces angiogenesis and inhibits tumor development. *FASEB J*. 2004;18:161–163.
21. Fan F, Stoeltzing O, Liu W, et al. Interleukin-1beta regulates angiopoietin-1 expression in human endothelial cells. *Cancer Res*. 2004; 64:3186–3190.
22. Wallace WC, Akar CA, Lyons WE, Kole HK, Egan JM, Wolozin B. Amyloid precursor protein requires the insulin signaling pathway for neurotrophic activity. *Brain Res Mol Brain Res*. 1997;52:213–227.
23. Drygin D, Barone S, Bennett CF. Sequence-dependent cytotoxicity of second-generation oligonucleotides. *Nucleic Acids Res*. 2004; 32:6585–6594.
24. Poulaki V, Qin W, Joussen AM, et al. Acute intensive insulin therapy exacerbates diabetic blood-retinal barrier breakdown via hypoxia-inducible factor-1alpha and VEGF. *J Clin Invest*. 2002;109: 805–815.
25. Usui T, Ishida S, Yamashiro K, et al. VEGF164(165) as the pathological isoform: differential leukocyte and endothelial responses through VEGFR1 and VEGFR2. *Invest Ophthalmol Vis Sci*. 2004; 45:368–374.
26. Neid M, Datta K, Stephan S, et al. Role of insulin receptor substrates and protein kinase C-zeta in vascular permeability factor/vascular endothelial growth factor expression in pancreatic cancer cells. *J Biol Chem*. 2004;279:3941–3948.
27. BenEzra D, Griffin BW, Maftzir G, Sharif NA, Clark AF. Topical formulations of novel angiostatic steroids inhibit rabbit corneal neovascularization. *Invest Ophthalmol Vis Sci*. 1997;38:1954–1962.
28. Moore JE, McMullen TC, Campbell IL, et al. The inflammatory milieu associated with conjunctivalized cornea and its alteration with IL-1 RA gene therapy. *Invest Ophthalmol Vis Sci*. 2002;43: 2905–2915.
29. Voronov E, Shouval DS, Krelin Y, et al. IL-1 is required for tumor invasiveness and angiogenesis. *Proc Natl Acad Sci USA*. 2003;100: 2645–2650.
30. Kuwano T, Nakao S, Yamamoto H, et al. Cyclooxygenase 2 is a key enzyme for inflammatory cytokine-induced angiogenesis. *FASEB J*. 2004;18:300–310.
31. Rabinovsky ED, Draghia-Akli R. Insulin-like growth factor I plasmid therapy promotes in vivo angiogenesis. *Mol Ther*. 2004;9:46–55.
32. Saijo Y, Tanaka M, Miki M, et al. Proinflammatory cytokine IL-1 beta promotes tumor growth of Lewis lung carcinoma by induction of angiogenic factors: in vivo analysis of tumor-stromal interaction. *J Immunol*. 2002;169:469–475.
33. Seo KH, Ko HM, Choi JH, et al. Essential role for platelet-activating factor-induced NF-kappaB activation in macrophage-derived angiogenesis. *Eur J Immunol*. 2004;34:2129–2137.
34. Yoshida S, Yoshida A, Matsui H, Takada Y, Ishibashi T. Involvement of macrophage chemotactic protein-1 and interleukin-1beta during inflammatory but not basic fibroblast growth factor-dependent neovascularization in the mouse cornea. *Lab Invest*. 2003; 83:927–938.
35. Kwon YW, Jang ER, Lee YM, et al. Insulin-like growth factor II induces interleukin-6 expression via NFkappaB activation in psoriasis. *Biochem Biophys Res Commun*. 2000;278:312–317.
36. Waters SB, Pessin JE. Insulin receptor substrate 1 and 2 (IRS1 and IRS2): what a tangled web we weave. *Trends Cell Biol*. 1996;6: 1–4.
37. Giovannone B, Scaldaferri ML, Federici M, et al. Insulin receptor substrate (IRS) transduction system: distinct and overlapping signaling potential. *Diabetes Metab Res Rev*. 2000;16:434–441.
38. Huang SS, Leal SM, Chen CL, Liu IH, Huang JS. Cellular growth inhibition by TGF-beta1 involves IRS proteins. *FEBS Lett*. 2004; 565:117–121.
39. Zheng B, Clemmons DR. Blocking ligand occupancy of the alphaV-beta3 integrin inhibits insulin-like growth factor I signaling in vascular smooth muscle cells. *Proc Natl Acad Sci USA*. 1998;95: 11217–11222.
40. Shaw LM. Identification of insulin receptor substrate 1 (IRS-1) and IRS-2 as signaling intermediates in the alpha6beta4 integrin-dependent activation of phosphoinositide 3-OH kinase and promotion of invasion. *Mol Cell Biol*. 2001;21:5082–5093.